

# Microstructure of Ti/Al ohmic contacts for *n*-AlGa<sub>N</sub>

S. Ruvimov,<sup>a)</sup> Z. Liliental-Weber, and J. Washburn  
Lawrence Berkeley National Laboratory, Berkeley, California 94720

D. Qiao and S. S. Lau  
University of California, San Diego, La Jolla, California 92093

Paul K. Chu  
City University of Hong Kong, Hong Kong

(Received 14 July 1998; accepted for publication 28 August 1998)

Transmission electron microscopy was employed to evaluate the microstructure of Al/Ti ohmic contacts to AlGa<sub>N</sub>/Ga<sub>N</sub> heterostructure field-effect transistor structures. Contact resistance was found to depend on the structure and composition of the metal and AlGa<sub>N</sub> layers, and on atomic structure of the interface. A 15–25-nm-thick interfacial AlTi<sub>2</sub>N layer was observed at the contact-AlGa<sub>N</sub> interface. Formation of such nitrogen-containing layers appears to be essential for ohmic behavior on *n*-type III-nitride materials suggesting a tunneling contact mechanism. Contact resistivity was found to increase with Al fraction in the AlGa<sub>N</sub> layer. © 1998 American Institute of Physics. [S0003-6951(98)01244-3]

GaN and related compounds are promising for high temperature/high power electronic devices<sup>1</sup> such as AlGa<sub>N</sub>/Ga<sub>N</sub> heterostructure field effect transistors (HFET). High quality ohmic contacts are critical to achieve a high transconductance and a high saturation current of HFETs.<sup>2</sup> For many practical applications contact resistance needs to be about 1 ohm mm or less. Several metallization schemes for ohmic contacts to *n*-Ga<sub>N</sub><sup>3–6</sup> and *n*-AlGa<sub>N</sub><sup>7</sup> with low contact resistivities have recently been reported. However, the mechanisms of the ohmic behavior are still under discussion.<sup>6–9</sup> Two models, low barrier Schottky or tunneling contact, have been proposed to explain ohmic behavior of metal contacts to *n*-type III nitrides.<sup>5,8</sup> The second mechanism involves the outdiffusion of nitrogen toward the metal layer and the formation of a heavily *n*-doped (by N vacancies) material, thus enhancing the possibility of carrier tunneling. Because this mechanism is, to some extent, independent of the particular metallization scheme, it could be applicable to various contacts.<sup>5,6,8</sup> The contact structure can be different even for similar metallization schemes.<sup>6,8,9</sup> Thus, further detailed structural studies are necessary for better understanding of ohmic contact behavior.

Here we report the results of high resolution and analytical electron microscopy studies of Al/Ti ohmic contacts to *n*-AlGa<sub>N</sub>/Ga<sub>N</sub> HFETs.

Typical AlGa<sub>N</sub>/Ga<sub>N</sub> HFET structures grown on (0001) sapphire substrates have a 1- $\mu$ m-thick insulating Ga<sub>N</sub> layer followed by a 3-nm-thick undoped Al<sub>0.15</sub>Ga<sub>0.85</sub>N layer and a 30-nm-thick doped Al<sub>0.15</sub>Ga<sub>0.85</sub>N layer. Al (71 nm)/Ti (30 nm) contacts were compared for four AlGa<sub>N</sub>/Ga<sub>N</sub> HFETs with different Al content in the AlGa<sub>N</sub> layer (see Table I). The Al concentration within AlGa<sub>N</sub> layers was estimated based on secondary ion mass spectroscopy (SIMS) and energy dispersive x-ray (EDX) spectroscopy measurements.

Contact resistance was measured by the transmission line method (TLM). The TLM samples were annealed in a flowing N<sub>2</sub> ambient at various temperatures up to 950 °C using a rapid thermal annealing. Details of the metallization scheme and surface treatment prior the metal deposition have been reported elsewhere.<sup>7</sup>

Transmission electron microscopy (TEM) studies were carried out on Topcon 002 and JEOL 200CX microscopes operated at 200 kV and on an ARM microscope operated at 800 kV. Cross-sectional specimens were prepared for TEM study by dimpling followed by ion milling.

The contact resistance and other pertinent parameters of AlGa<sub>N</sub>/Ga<sub>N</sub> HFETs are summarized in Table I. The contact resistivity gradually increases from sample No. 11 to No. 8 in Table I along with Al content and the thickness of the AlGa<sub>N</sub> layer indicating a correlation between the contact resistance and the composition of the AlGa<sub>N</sub> layer. Although SIMS and EDX data on the Al content differ by a few at. %, both techniques show the same trend, an Al fraction increases from sample No. 11 to No. 8. This shows that significant variations in Al content occur within AlGa<sub>N</sub> layers for nominally identical AlGa<sub>N</sub>/Ga<sub>N</sub> HFETs. The two AlGa<sub>N</sub>/Ga<sub>N</sub> structures, Nos. 7 and 9 in Table I, were grown using the same process, but still differ in Al fraction in the AlGa<sub>N</sub> layer and in the sheet charge mobility product ( $n_s\mu$ ). Despite nominally identical growth conditions of the AlGa<sub>N</sub>/Ga<sub>N</sub> HFETs and the same metallization scheme, the contact resistances were found to differ by a few orders of magnitude after high temperature annealing. In order to understand an effect of Al content in the AlGa<sub>N</sub> layer on contact resistance, the microstructure of the contacts was studied by high resolution electron microscopy (HREM).

Figure 1(a) shows a typical cross-section electron microscopy image of a Ti/Al contact to an AlGa<sub>N</sub>/Ga<sub>N</sub> HFET structure after annealing at 950 °C for 80 min. The contact layer contains two sublayers of different contrast due to different Al/Ti ratio in the sublayers. EDX analysis (not shown) evidences that the composition of the top sublayer is close to

<sup>a)</sup>On leave from A.F. Ioffe Physico-Technical Institute, St. Petersburg 194021, Russia. Electronic mail: ruv@mhl1.lbl.gov

TABLE I. Contact resistance and parameters of AlGaIn/GaN HFET structures under study.

Samples	$n_s, \mu 10^{16}$ , 1/V s	$R_s$ , $\Omega \text{ cm}^2$	Al concentration in AlGaIn layer, %		Thickness of AlGaIn layer, nm		Interface roughness, nm
			SIMS	EDX	SIMS	TEM	
No. 11	1.20	$8.60 \times 10^{-7}$	9	11–15.2	22	21	2.7
No. 9	0.74	$4.00 \times 10^{-6}$	10	~25.3	36	28	2.0
No. 7	1.09	$2.05 \times 10^{-4}$	15	22–25.4	36	28	6.0
No. 8	1.34	$2.07 \times 10^{-3}$	22	30	60	34	5.5

$R_s$  is a specific contact resistivity.

$\text{Al}_3\text{Ti}$  in good agreement with previous results,<sup>7,8</sup> while the interfacial layer (with darker contrast) is rich in Ti (with Ti/Al~2). A high resolution electron microscope (HREM) image of the interfacial layer is shown in Fig. 1(b). The lattice parameters of the Ti-rich layer evaluated from the electron diffraction pattern (not shown) and HREM image of Fig. 1(b) ( $a = 0.296 \pm 0.01 \text{ nm}$ ,  $c = 1.43 \pm 0.03 \text{ nm}$ ) are close to those taken from crystallographic tables<sup>10</sup> for the hexagonal  $\text{Ti}_2\text{AlN}$  phase ( $a = 0.299 \text{ nm}$ ,  $c = 1.361 \text{ nm}$ ). Computer simulation of HREM images (not shown) for this hexagonal  $\text{Ti}_2\text{AlN}$  phase reproduces a distinct feature of the experimental image of Fig. 1(b) where every third monolayer is highlighted. Electron energy loss spectroscopy (not shown) confirms the presence of nitrogen in the interfacial layer. The orientation relationship between the  $\text{AlTi}_2\text{N}$  and the AlGaIn was found to be:  $(0001)_{\text{AlTi}_2\text{N}} \parallel (0001)_{\text{AlGaIn}}$ ,  $(11\bar{2}0)_{\text{AlTi}_2\text{N}} \parallel (11\bar{2}0)_{\text{AlGaIn}}$ .

The presence of nitrogen in the interfacial layer suggests the reaction of Ti with AlGaIn and possible outdiffusion of nitrogen from the III-nitride material rather than nitrogen diffusion from ambient through the Al or  $\text{Al}_3\text{Ti}$  layers. Indeed, no AlN, TiN, or Ti–Al–N phases have been detected in the contact far from the interface. A similar process was considered for the formation of nitrogen-containing layers (TiN<sup>8</sup> or AlN<sup>6</sup>) at the interface of Al/Ti contacts to  $n$ -GaIn after high temperature annealing. The reaction of Ti with AlGaIn during annealing was clearly demonstrated in the case of W/Al/Ti contacts, rich in Ti, where AlGaIn was partly or, sometimes, completely consumed by the reaction.<sup>11</sup> Nitrogen outdiffusion from III-nitride material can result in a N-deficient layer underneath the reacted layer.

This N-deficient layer is believed to be highly doped  $n$ -type material, resulting in the observed ohmic behavior due to carrier tunneling across the metal III-nitride junction.<sup>5,8</sup> Tunneling should be rather independent of the work function of the interfacial layer. This might explain why ohmic behavior has been reported for several different metal contacts to  $n$ -GaIn including Al,<sup>6</sup> Pd/Al,<sup>6,9</sup> and Ti/Al.<sup>6</sup> Contact quality has been shown to depend on many factors (the substrate treatment prior to the metal deposition such as surface cleaning, reactive ion etching and substrate pre-annealing, the metallization scheme, and the annealing conditions). However, the nitrogen-containing layer (TiN or AlN) at the interface was a common feature for all those contacts to  $n$ -GaIn suggesting the tunneling mechanism for ohmic contacts to  $n$ -AlGaIn. A similar mechanism can be expected for ohmic Al/Ti contacts to  $n$ -AlGaIn.

However, the doping efficiency for N vacancies in Al-

GaIn is expected to be lower compared to GaN due to the increase of the band gap. This might lead to an increase of contact resistance with Al fraction in the AlGaIn layer assuming a tunneling contact mechanism. Another possible reason for the increase of contact resistivity with Al content could be electron confinement at the AlGaIn/GaN interface due to the piezoelectric effect.<sup>12</sup> In any case, increase of the contact resistivity with Al content in AlGaIn layer seems to be a generic problem. Therefore, in order to decrease the contact resistivity the AlGaIn layer under the ohmic contact should either be heavily doped (e.g., by ion implantation of Si) or substituted by GaN (e.g., removing of AlGaIn in the contact area by etching followed by selective growth of GaN prior to contact deposition).<sup>12</sup>

Based on our observations, the following scenario for solid state reactions in Al/Ti contacts to AlGaIn during annealing is suggested. The reactions first start between Al and Ti at rather low temperatures (in the range of 250–300 °C) with the formation presumably of the  $\text{Al}_3\text{Ti}$  phase as expected according to the binary Al–Ti phase diagram. Its formation was also confirmed by Rutherford backscattering (RBS) measurements.<sup>7</sup> Formation of an  $\text{Al}_3\text{Ti}$  layer from individual Al and Ti layers requires the Al/Ti thickness ratio to be equal to 2.82 taking into account the densities of Ti and Al metals. The Al/Ti ratio was about in 2.37 for samples in the present study, suggesting an excess of Ti (of about 5 nm) reacting with the AlGaIn. The reaction of Ti with AlGaIn which starts probably above 400 °C results, first, in the dissolution of the native oxide from the AlGaIn surface and, then, in the outdiffusion of N and the formation of the Ti–Al–N interfacial phase. Decomposition of the AlGaIn that happens probably at higher temperatures (above 850 °C) leads to formation of the  $\text{Ti}_2\text{AlN}$  phase at the interface. Partial decomposition of the AlGaIn results in the outdiffusion of Ga and, sometimes, in the formation of small pockets at the interface (not shown), especially, at higher temperatures

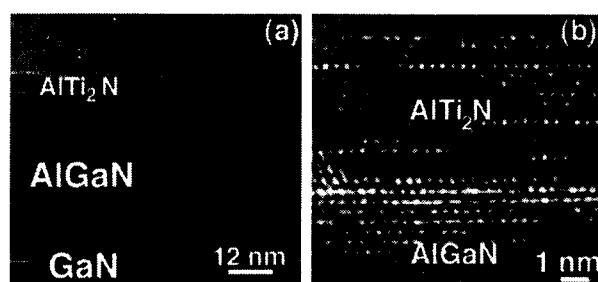


FIG. 1. Typical cross-sectional TEM (a) and HREM (b) images of Al/Ti metal contact (sample No. 9 in Table I) to AlGaIn/GaN.

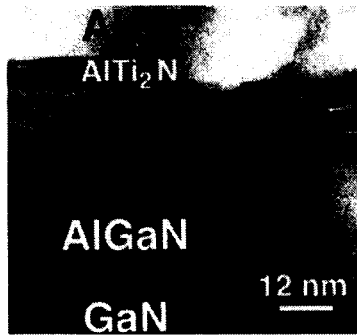


FIG. 2. Cross-sectional TEM image of Al/Ti metal contact to AlGaIn/GaN with rough interface (sample No. 7 in Table I).

and longer time of annealing. Those pockets and interface roughness, associated with them, might be responsible for the increase of contact resistivity observed for high temperature annealing of nonpreannealed samples in Ref. 7 (see, e.g., Fig. 3 in Ref. 7). The presence of Ga in the metal layer after annealing was detected by both EDX and SIMS measurements. Ga is expected to outdiffuse toward the surface and form the deposits there. The formation of a  $Ti_2AlN$  layer at the interface with AlGaIn and partial decomposition of AlGaIn associated with it have also been observed for W/Al/Ti contacts to AlGaIn/GaN HFETs after high temperature annealing.<sup>11</sup>

Because AlN appears to be more stable than GaN (the activation energies for nitrogen dissociation from the surface are about 4.4 and 3.8 eV for AlN and GaN, respectively),<sup>13</sup> the stability of AlGaIn at high temperatures increases with Al content. As a result, the sputtering rate in SIMS decreases with increasing Al content which leads to the overestimation of the thickness of the AlGaIn layer based on SIMC measurements (see Table I). This also suggests that Al might create a barrier for the outdiffusion of N and, hence, for the reaction between Ti and AlGaIn. Fluctuations of Al composition over the AlGaIn layer and/or the effect of defects would lead to roughening of the reaction front during annealing of Al/Ti contacts, especially at higher Al concentrations. This might lead to increase in interface roughness for contacts to AlGaIn with increase in Al content as observed in our study (see Table I). Indeed, the low resistance contact [Fig. 1(a)] has a uniform interfacial layer over all the visible area and an abrupt interface with the AlGaIn (the interface roughness is about 2 nm), while the interfacial layer in the high resistance contact (Fig. 2) is often discontinuous and has a rough interface (about 6 nm). The observed correlation between interface roughness and contact resistance might also suggest an increase of contact resistivity with interface

roughness, but the mechanism of this effect is not clear yet. However, interface roughness probably has less effect on the contact resistivity than the composition of the AlGaIn layer in the present study. Similarly, W/Al/Ti contacts to AlGaIn were found to have a low specific resistance (about  $8 \times 10^{-6} \Omega \text{ cm}^2$ ) despite the rough interface with AlGaIn.<sup>11</sup>

In conclusion, the formation of ohmic contacts appears to be a complex process that includes solid state reactions at the interface with the substrate. These reactions have been shown to result in a nitrogen-containing interfacial layer and in the formation of a heavily doped layer (probably rich in N vacancies) thus enhancing the possibility of carrier tunneling. Contact resistance was found to depend on the metallization scheme, the Al fraction in the AlGaIn layer, and the atomic structure of the metal/AlGaIn interface. Contact resistivity increases with Al fraction in the AlGaIn layer.

This study was supported by BMDO (Dr. K. Wu) monitored by the USA Space Missile and Strategic Defense Command (order N W31RPD-8-A8015) through U.S. DOE under Contract No. DE-AC03-76SF00098. The use of the facilities at National Center for Electron Microscopy and assistance of W. Swider for sample preparation are gratefully acknowledged. UCSD also acknowledges the partial financial support from NSF.

<sup>1</sup>S. N. Mohammad, A. Salvador, and H. Morkoç, Proc. IEEE **83**, 1306 (1995).

<sup>2</sup>M. Asif Khan, M. S. Shur, and Q. Chen, Appl. Phys. Lett. **68**, 3022 (1996).

<sup>3</sup>M. E. Lin, Z. Ma, F. Y. Huang, Z. F. Fan, L. H. Allen, and H. Morkoç, Appl. Phys. Lett. **64**, 1003 (1994).

<sup>4</sup>J. D. Guo, C. I. Lin, M. S. Feng, F. M. Pan, G. C. Chi, and C. T. Lee, Appl. Phys. Lett. **68**, 235 (1996).

<sup>5</sup>Z.-F. Fan, S. N. Mohammad, W. Kim, O. Aktas, A. E. Botchkarev, and H. Morkoç, Appl. Phys. Lett. **68**, 1672 (1996).

<sup>6</sup>B. P. Luther, S. E. Mohny, T. N. Jackson, M. Asif Khan, Q. Chen, and J. W. Yang, Appl. Phys. Lett. **70**, 57 (1997).

<sup>7</sup>Q. Z. Lui, L. S. Yu, F. Deng, S. S. Lau, Q. Chen, J. W. Yang, and M. A. Khan, Appl. Phys. Lett. **71**, 1658 (1997).

<sup>8</sup>S. Ruvimov, Z. Liliental-Weber, J. Washburn, K. J. Duxstad, E. E. Haller, Z.-F. Fan, S. N. Mohammad, W. Kim, A. E. Botchkarev, and H. Morkoç, Appl. Phys. Lett. **69**, 1556 (1996); S. Fonash, S. Ashok, and R. Singh, *39*, 423 (1981).

<sup>9</sup>B. P. Luther, J. M. DeLucca, S. E. Mohny, and R. F. Karlicek, Jr., Appl. Phys. Lett. **71**, 3859 (1997); D. W. Jenkins and J. D. Dow, Phys. Rev. B **39**, 3317 (1989).

<sup>10</sup>P. Villars and L. D. Calvert, *Pearson's Handbook of Crystallographic Data for Intermetallic Phases*, 2nd ed. (ASM, Materials Park, 1991), Vol. 1, p. 933.

<sup>11</sup>S. Ruvimov, Z. Liliental-Weber, J. Washburn, D. Qiao, Q. Z. Lui, and S. S. Lau, in Proc. of SIMC-X, 1998 (unpublished).

<sup>12</sup>U. K. Mishra, in Proc. of SIMC-X, 1998 (unpublished).

<sup>13</sup>X. A. Cao, C. R. Abernathy, R. K. Singh, S. J. Pearton, M. Fu, V. Sarvepalli, J. A. Sekhar, J. C. Zolper, D. J. Rieger, J. Han, T. J. Drummond, R. J. Shul, and R. G. Wilson, Appl. Phys. Lett. **73**, 229 (1998).